IChemE

0263–8762/98/$10.00+0.00

Trans IChemE, Vol 76, Part A, February 1998

MODELLING OF HEAT TRANSFER IN RADIATING AND COMBUSTING SYSTEMS

M. G. CARVALHO and T. L. FARIAS

Instituto Superior Tecnico, Mechanical Engineering Department, Technical University of Lisbon, Portugal

The solution of reactive flow problems with radiative heat transfer requires a radiation model which is simultaneously accurate, fast and compatible with the algorithm employed to solve the transport equations. In the present paper, a review of the most commonly used methods to predict radiative heat transfer in combustion chambers is presented. Among them, three methods that satisfy the above requirements are described in more detail; namely the discrete transfer, the discrete ordinates and the finite volume method. Some examples of results obtained for simple test cases are presented where predictions obtained with some of the most well known models are compared. An important issue within the radiation modelling domain is the evaluation of the radiative properties of gases and particulate matter that are commonly found in the combustion products. Therefore, in the second part of the paper, the problems related to the evaluation of the radiative properties of the combustion products, i.e. participating gaseous species and particles, are focused and the methods used to solve these problems are described.

Keywords: radiation heat transfer; radiation modelling; radiative properties of combustion products

1. INTRODUCTION

Radiative heat transfer plays an important role in several engineering problems, namely in aeronautics, astronautics and mechanics, and it is the dominant heat transfer mechanism in many industrial combustion equipment, including boilers and furnaces. Hence, the accurate prediction of the heat transferred by radiation is a key issue in the design and operation of combustion chambers. In this case, the calculation of radiative heat transfer is part of a more complex problem which involves the numerical simulation of a turbulent reactive flow. Based on these considerations, the study of energy transfer through media that can absorb, emit and scatter has received increased attention in the past two decades. This interest stems from the complicated and interesting phenomena associated with combustion chambers at high temperatures where radiation heat transfer plays a dominant role. The difficulty in the exact calculation of multidimensional radiative transfer in absorbing-emitting and scattering media has led researchers to develop approximate schemes.

In the present paper, a review of the most commonly used methods to predict radiative heat transfer in combustion chambers is presented. Their advantages and disadvantages are discussed and a comparison between their performance for several test cases is presented. Further on, attention is given to the methods used in engineering problems to predict the radiative properties of the combustion products.

2. THE RADIATIVE HEAT TRANSFER EQUATION

The radiative transfer equation (RTE) is a mathematical statement of the conservation principle applied to a pencil of radiation (ray) travelling along a path through a medium. Radiation travelling along a path is attenuated by absorption and scattering (out scattering), and is enhanced by emission and by radiation in-scattered from other directions. All these effects can be easily detected in the RTE—see, e.g. Siegel and Howell[1] and Modest[2]. The radiative transfer equation can be expressed as:

$$\frac{\mathrm{d}I_\lambda}{\mathrm{d}s} = -(\kappa_\lambda + \kappa_{\lambda s})I_\lambda + \kappa_\lambda I_{b\lambda} + \frac{\kappa_{\lambda s}}{4\pi}\int_0^{+\infty}\int_0^{4\pi} \Phi\left(\vec{s}' \rightarrow \vec{s}; \lambda' \rightarrow \lambda\right) I'_\lambda\left(\vec{s}'\right)\mathrm{d}\Omega'\mathrm{d}\lambda' \qquad (1)$$

where I_λ is the spectral radiation intensity, $I_{b\lambda}$ is the spectral radiation intensity for a black body, κ_λ is the spectral absorption coefficient of the medium, $\kappa_{\lambda s}$ is the spectral scattering coefficient and $\Phi(s' \rightarrow \vec{s}, \lambda' \rightarrow \lambda)\mathrm{d}\Omega'\mathrm{d}\lambda'/4\pi$ represents the probability that radiation of wavelength λ' propagating in the direction $\vec{s}'$ and confined within the solid angle $\mathrm{d}\Omega'$ is scattered to the direction $\vec{s}$ and wavelength 1. On the right hand side the first term represents the loss of energy by absorption and out-scattering, followed by the gain of energy due to emission and the last term represents the gain of energy by in-scattering. For the particular case where the combustion products do not scatter light we have $\kappa_{\lambda s} = 0$ and integration of equation 1 over all wavelengths yields:

$$\frac{\mathrm{d}I}{\mathrm{d}s} = \kappa I + \frac{\kappa\sigma T_g^4}{\pi} \qquad (2)$$

Two major difficulties may easily be identified in the analysis of the RTE (equation (1)). First, the RTE is an integro-differential equation and an exact solution may only

be obtained after simplifying assumptions such as uniform radiative properties of the medium and homogeneous boundary conditions. Additionally, most engineering systems are multidimensional, the medium is not homogeneous and radiative properties are spectral in nature. Therefore, it can be concluded that the exact solutions for the RTE are not practical for engineering applications. The second problem deals with the evaluation of all the coefficients (scattering and absorption coefficients of the combustion products; shape of the phase function) present in the RTE which depend on wavelength, gas composition, temperature, pressure, type of particles, etc. These two main problems may be partially eliminated through the use of models capable, in one hand, of simplifying the integro-differential equations that need to be solved, and, on the other hand, to predict the radiation properties of the combustion products with a similar accuracy.

In the next section, special attention will be given to the most common methods developed to solve the radiation heat transfer inside the combustion chamber, namely the zone model, the Monte Carlo method and the flux methods, amongst others. Three of the most attractive methods, as far as accuracy and computational requirements are concerned (as well as the flexibility to be incorporated in reactive fluid flow codes), are the discrete transfer[3,4], the discrete ordinates[5,6] and the finite volume method[7,8]. A more detailed description of these methods is included in the next section. In the following section results obtained using the most popular models previously mentioned are compared for simple test cases. Section 5 will be dedicated to the methods used in most engineering problems to evaluate the radiation properties of combustion products while major conclusions are summarized in the final section.

3. SOLUTION METHODS

The RTE is an integro-differential equation, and its exact solution can only be obtained for very simple cases, such as one-dimensional problems or when uniform radiative properties of the medium and homogeneous boundary conditions are assumed. Crosbie and Dougherty[9] presented a detailed review of one-dimensional exact solution methods. Exact solutions for multi-dimensional cases have been presented in the literature[10–13]. Most engineering systems are multidimensional and spectral variation of the radiative properties must be accounted for when solving the RTE if accurate predictions are desired. Therefore, the exact solutions for RTE are not practical for engineering applications. Consequently, it is necessary to introduce simplifying assumptions before attempting to solve the radiative heat transfer problem. During the last few decades numerous methods to solve the RTE have been developed. A survey of the literature published over the past years is presented, for example, by Viskanta and Menguç[14], Howell[15] and Modest[2].

Zone Method

The zone method (also known as zoning method, zonal method or, most frequently as Hottel's zonal method), presented by Hottel and Cohen[16] and Hottel and Sarofim[17], is probably the most used method to predict radiative heat transfer in combustion chambers. In this method, the system is divided into surface zones and gas zones. Direct exchange factors for gas–gas, gas–surface, and surface–surface zone interchange have to be available or calculated. Knowing the values of these factors, it is possible to calculate the net exchange factor for any pair of zones. The resultant factors are used to form a set of energy balances, one for each zone, and, by simultaneous solution, the gas and surface space temperature distributions and the heat fluxes along the surfaces are determined.

Although simple and very attractive, the zone method has several limitations. Firstly, for complex geometries, the direct exchange factors are frequently not available and its evaluation may become impractical. Secondly, it is difficult to couple the zonal method solution procedure with the flow field and energy equations which are usually solved using finite difference (or finite element) techniques. However, it should be mentioned that the computer time required by the present method is usually smaller that the time consumed by its most direct alternatives. The zone method has been extensively used to predict the radiative heat transfer in three-dimensional rectangular enclosures[18–21]. For cylindrical geometries, the zone method was applied, for example, by Steward and Cannon[22], Wu and Fricker[23], Heap *et al.*[24] and Selçuk *et al.*[25].

Monte Carlo Method

The Monte Carlo Method, Howell and Perlmuter[26], is a statistical method. Although there are many different versions of Monte Carlo methods, they are all based on following the probable path of a discrete bundles of energy, the 'photon', until their final absorption in the system (wall or gas). Usually the path is determined at each point of emission, reflection or absorption by a random choice from the possible paths. This choice takes into account the radiative properties of the medium and the walls. The energy emitted from the surface is related to the number of bundles originating from that surface. After leaving the surface, the photon may be absorbed by the gas (determined by a random choice based on the gas absorption coefficient). In that case, a new photon is sent with a new randomly chosen direction (based on the scattering characteristics of the gas). If it is not absorbed by the gas, the photon will reach a wall. Here a random choice, taking into account the surface absorptivity, will determine whether the photon is absorbed or reflected. If the former happens, the ray's history is terminated. If it is reflected, the new direction is chosen by a random choice. Heat balance of the surfaces and gas are related to the number of photons absorbed versus those emitted.

To have some statistical significance, a large enough sample of energy bundles must be followed. The Monte Carlo method can easily be used for any complex geometry. In principle, as the number of photons followed increases to infinity, the method should converge to the exact solution. Nevertheless, the results obtained with this method are always affected by a statistical error. Although the present method is very flexible, its major disadvantage is once again related to the compatibility problem with the solution method used to solve the flow equations. The Monte Carlo method has been successfully employed to solve radiation heat transfer problems in multi-dimensional enclosures and furnaces[22,27].

Flux Methods

Flux models are based on the use of some simplifying assumption for the angular variation of the radiation intensity at any point. The mathematical model of the radiation field at the point then takes the form of a set of simultaneous partial differential equations with respect to positions in terms of the unknown parameters in the approximate angular representation of intensity variation. The flux models have emerged from studies in Astro and Nuclear Physics. In these fields these methods were mainly used in a one-dimensional form. It was only in the early seventies that the flux models attracted the interest of combustion engineers and they were extended to two and three-dimensional situations.

Schuster-Hamaker Type of Models

Models of this type (see Hamaker[28]) use the simplest and least accurate representation of the intensity variation: plane parallel radiation is assumed in each dimension. For each dimension, two differential equations are produced by carrying out radiative energy balances for forward and backward directions. The four-flux model of Gosman and Lockwood[29] and the six-flux models of Patankar and Spalding[30] are of this kind.

Schuster-Schwarzschild Type of Models

The basis of these models is to subdivide the total solid angle surrounding a point into smaller solid angles in each of which intensity is assumed to be uniform—see Abramzom and Lisin[31]; Spalding[32]. Discontinuous changes in intensity occur in passing from one smaller solid angle to any adjacent smaller solid angle. Integration of the equation of radiant energy transfer for each smaller solid angle, in turn, produces a group of partial differential equations in the unknown intensities. Four-flux models of Schuster-Schwarzschild type for axisymmetrical radiation fields were proposed by Lowes *et al.*[20], Richter and Quack[21] and Siddal and Selçuk[33]. A six-flux model of the same type for three-dimensional radiation field was proposed by Siddal and Selçuk[34]. For an absorbing, emitting and scattering medium, Spalding[32] suggested a similar six-flux model for cylindrical geometries.

Spherical Harmonic Models

An elegant way of avoiding the solution of the integro-differential RTE is through the use of expansions of the local intensity in terms of spherical harmonics, with truncation to N terms in the series, and substitution into the moments of the differential form of the equation of transfer. This approach leads to the *P-N* approximations, see Jeans[35] and Viskanta[36], where N is the order of the approximations. As N approaches infinity, the solutions obtained became exact. Usually, odd orders are employed, especially $P1$ and $P3$. Going to $P5$, an additional increase in accuracy is obtained, while the complexity of the calculations becomes more cumbersome. The reasons for avoiding even orders are discussed by Viskanta and Menguç[14] and Howell[15]. The accuracy of the Spherical Harmonic model for axisymmetrical radiation fields were tested by various researchers[37,38].

Discrete Ordinates Approximations

The discrete ordinates method[39] relies on a discrete representation of the directional dependence of the radiation intensity. The total solid angle surrounding each point is subdivided into smaller solid angles in each of which a direction for the intensity is specified. Application of equation of radiant energy transfer into each direction produces differential equations in terms of the unknown intensities in the specified directions—see Chandrasekhar[39] and Truelove[40]. For the particular case of non-scattering media, equation 2 may be written as follows for any discrete direction $\vec{s}_i$:

$$\xi_i \frac{\partial I_i}{\partial x} + \eta_i \frac{\partial I_i}{\partial y} + \mu_i \frac{\partial I_i}{\partial z} = -\kappa I_i + \kappa I_b \tag{3}$$

where ξ_i, η_i and μ_i are the direction cosines of direction i and I_b is the total black-body radiation intensity. This equation is integrated over each control volume, yielding a relationship between the volume average intensity, I_{P_i}, and the radiation intensities entering (subscript i) and leaving (subscript e) the control volume:

$$I_{Pi} = \frac{\kappa V \gamma I_{bi} + |\xi_i| A_x I_{x_i,i} + |\eta_i| A_y I_{y_i,i} + |\mu_i| A_z I_{z_i,i}}{\kappa V \gamma + |\xi_i| A_x + |\eta_i| A_y + |\mu_i| A_z} \tag{4}$$

In this equation, V stands for the volume of the cell and A_x, A_y and A_z denote the areas of the cell faces normal to directions x, y and z, respectively. The parameter γ relates the incoming and outgoing radiation intensities to the volume average intensity according to the following relations:

$$I_{Pi} = \gamma I_{x_{e,i}} + (1-\gamma) I_{x_{i,j}} \tag{5a}$$

$$I_{Pi} = \gamma I_{y_{e,i}} + (1-\gamma) I_{y_{i,i}} \tag{5b}$$

$$I_{Pi} = \gamma I_{z_{e,i}} + (1-\gamma) I_{z_{i,i}} \tag{5c}$$

The most common values of γ are $\gamma = 1/2$ (diamond scheme) and $\gamma = 1$ (step scheme). The boundary conditions may be written as follows:

$$I_i = \varepsilon_w I_{bw} + \frac{1-\varepsilon_w}{\pi} \sum_{\xi_j<0} w_j I_j |\xi_j| \tag{6}$$

where w_j is the quadrature weight associated with the direction j.

The numerical solution of equation (4) is carried out starting from one of the corners of the computational domain, depending on the sign of the direction cosines. In each iteration, and for each one of the selected directions, the radiosity of the boundaries and the internal radiation sources in each cell are either known or guessed from the values computed in the previous iteration. Hence, all the control volumes are visited to compute the radiation intensities I_{P_i} according to equation (4) and using the auxiliary relations (5a–c). After all the directions have been treated, the radiosities of the boundaries and the radiation sources may be updated and the iteration process continues until the convergence criterion has been achieved. The extrapolation of the outgoing intensities according to equations (5a–c) may yield negative intensities if $\gamma < 1$, which is not physically realistic. To minimize this problem, the radiation intensities are set to zero in such a case and I_{P_i} is recalculated. In this way no negative intensities appear, although numerical oscillations in the solution may still arise.

The finite volume method

The finite volume method[7,8] has many similarities with the discrete ordinates method. The magnitude of radiation intensity is also assumed constant in each discrete direction, and the radiative transfer equation is solved for a set of discrete directions which span the total solid angle of 4π. However, to obtain the discrete equations, the radiative transfer equation is integrated over each control volume and over each solid angle in which the space is discretized:

$$\int_{\Delta\Omega_i}\int_{\Delta V}\frac{\mathrm{d}I_i}{\mathrm{d}s}\mathrm{d}V\ \mathrm{d}\Omega_i = \int_{\Delta\Omega_i}\int_{\Delta V}(-\kappa I + \kappa I_b)\mathrm{d}V\ \mathrm{d}\Omega_i \tag{7}$$

Applying the Gauss divergence theorem, this equation reads as:

$$\int_{\Delta\Omega_i}\int_{\Delta A} I_i(\vec{s}_i.\vec{n})\mathrm{d}A\ \mathrm{d}\Omega_i = \int_{\Delta\Omega_i}\int_{\Delta V}(-\kappa I + \kappa I_b)\mathrm{d}V\mathrm{d}\Omega_i \tag{8}$$

Whereas in the discrete ordinates method the direction $\vec{s}_i$ is taken as a constant within the solid angle $\Delta\Omega_i$, in the finite volume method it varies, following the variation of the polar angle θ and the azimuthal angle ϕ within $\Delta\Omega_i$. Therefore, a different discretized equation is obtained, which may be written as follows:

$$I_{P_i} = \frac{\gamma\kappa I_b V\Delta\Omega_i + D_{i,cx}A_x I_{x_i,i} + D_{i,cy}A_y I_{y_i,i} + D_{i,cz}A_z I_{z_i,i}}{\gamma\kappa V\Delta\Omega_i + D_{i,cx}A_x + D_{i,cy}A_y + D_{i,cz}A_z} \tag{9}$$

where

$$D_{i,cx} = \int_{\Delta\Omega_i}\vec{s}_i.\vec{i}\,\mathrm{d}\Omega_i, \quad D_{i,cy} = \int_{\Delta\Omega_i}\vec{s}_i\vec{j}\ \mathrm{d}\Omega_i,$$

$$D_{i,cz} = \int_{\Delta\Omega_i}\vec{s}_i.\vec{k}\ \mathrm{d}\Omega_i \tag{10}$$

and

$$\Delta\Omega_i = \int_{\Delta\phi_i}\int_{\Delta\theta_i}\mathrm{sen}\,\theta\,\mathrm{d}\theta\,\mathrm{d}\phi \tag{11}$$

The discrete ordinates equation (4) would be recovered from (9) by replacing $D_{i,cx}$, $D_{i,cy}$ and $D_{i,cz}$ by $|\xi_i|$, $|\eta_i|$ and $|\mu_i|$, respectively, and by deleting $\Delta\Omega_i$ from the numerator and the denominator. The boundary conditions may be written as follows:

$$I_i = \varepsilon_w I_{bw} + \frac{1-\varepsilon_w}{\pi}\sum_{\vec{s}_j.\vec{n}<0} I_j\int_{\Delta\Omega_i}|\vec{s}_j.\vec{n}|\,\mathrm{d}\Omega_i \tag{12}$$

where $\vec{n}$ denotes the normal to the boundary. The solution procedure is similar to that described for the discrete ordinates method.

The flux methods previously presented have several advantages. The extension to these methods to include anisotropic scattering is straightforward, which is a very useful tool in modelling combustion systems where the presence of particles is an important factor. Additionally, these models have also been used widely because the differential form of the resulting radiative transfer equations makes them compatible with the algorithm used for the flow and energy equations simulation.

Hybrid Methods

The methods discussed in this section present some disadvantages. In order to avoid these disadvantages, and additionally use the desirable characteristics of the different models, several hybrid radiative transfer models have been developed during the last few years. One of them is the Discrete Transfer model, a method that has its origin in the flux model but also exhibits features of the Hottel zone and Monte Carlo techniques. Presented by Lockwood and Shah[4], it was specially developed for predicting radiative heat transfer in combustion chambers.

The discrete transfer method

The discrete transfer method[3,4] is based on the solution of equation (2) along specified directions. The physical domain is divided into control volumes and the temperature and absorption coefficient of the medium are taken as constant in each one of them. Then, the central point P of each cell on the boundary is determined and a semihemisphere centred in P is considered and subdivided into a given number of solid angles. Each solid angle defines a direction along which the radiative transfer equation is solved. Hence, given a point P at the centre of a cell face on the boundary, a radiation beam is fired from P for each one of the directions selected above. The path of a radiation beam is followed until it hits another boundary. Let Q_i be the impingement point. Although, in general, Q_i is not the central point of a boundary cell, it is assumed that the radiation intensity at Q_i and at the central point of the cell containing Q_i are equal. Then, starting from Q_i, the path of the beam is followed back to the origin P and the radiative heat transfer equation is integrated analytically along this path yielding:

$$I_{n+1} = I_n e^{-\kappa\delta} + \frac{\sigma T_g^4}{\pi}(1 - e^{-\kappa\delta}) \tag{13}$$

where δs is the distance travelled by the radiation beam within the control volume, and I_n and I_{n+1} are the radiation intensities entering and leaving the control volume, respectively. The incident radiative heat flux at point P, G_p, is calculated by adding up the contributions due to all the radiation beams that reach point P:

$$G_P = \sum_i I_{PQ_i}\left(\vec{\Omega}_{PQ_i}.\vec{n}\right)\Delta\Omega_{PQ_i} \tag{14}$$

where the summation extends over all those beams, one for each solid angle resulting from the discretization of the semihemisphere centred in P. In this equation, Ω_{PQ_i} denotes the unit vector along the direction defined by P and Q_i, and $\vec{n}$ is the unit vector normal to the wall in point P.

The solution of the radiative heat transfer requires as a boundary condition knowledge of the wall temperature distribution or heat fluxes at the walls. If the wall temperature is prescribed, the boundary condition may be written as:

$$J_P = \varepsilon_w\sigma T_w^4 + (1-\varepsilon_w)G_P \tag{15}$$

where J_P is the radiosity in point P and ε_w is the wall emissivity. The calculation procedure is iterative, unless

$\varepsilon_w = 1$, because the radiation intensities at the starting points Q_i, given by J_{Q_i}/π, are not known a priori.

The Discrete Transfer method presents several advantages, namely: it is flexible (complicated geometries can be easily handled); it is easy to control the accuracy and the computer time required through the variation of the number of rays used (keeping the same grid), without increasing storage; and it is easily used for Cartesian, cylindrical or spherical coordinates—the form of the equation to be solved is exact the same; only the calculations of the intersections between rays and cells is different.

Due to the aforementioned advantages the Discrete Transfer method has been employed, together with solutions of the flow equations, to address a variety of problems such as computing the performance of industrial glass furnaces[41–44], calculating the working conditions of a gas turbine combustor[45] and predicting the performance of a pulverized fuel fired furnace[46–48].

There are some constraints attached to the Discrete Transfer model. The more notorious one is related with the difficulty of extending the model to anisotropic scattering problems. Nevertheless, for isotropic situations, the Discrete Transfer method presents very good results, as reported by Carvalho *et al.*[49,50]. In addition, the discrete transfer method is not conservative which is a disadvantage when coupling the method to a CFD code where the governing equations are often solved using a finite volume method which is conservative. The reason for this behaviour has been examined by Coelho and Carvalho[51] and a conservative formulation has been proposed and evaluated by those authors.

4. COMPARISON OF METHODS

Several authors have published comparisons between the performance of different radiative models using simple test cases or experimental data (References 14, 50 and 52, and the references cited therein). In this section, a few examples are reviewed in order to highlight the potentialities of the different models addressed.

Two dimensional rectangular enclosure

In the first test case, a two-dimensional square enclosure with black walls and zero emissive power was studied. The absorption coefficient of the medium is $\kappa = 1\ m^{-1}$ and the emissive power is one. Calculations were performed using a grid with 10×10 control volumes. The results reported were published by Coelho *et al.*[52]. The numerical solutions obtained by those authors for the Discrete Transfer, Discrete ordinates and Finite Volume method are shown in Figure 1. For the Discrete Transfer method, 2×5 rays were used per octant; Discrete Ordinates results were obtained using an S8 approximation, while the same number of directions were also used for the Finite Volume calculations. Results in Figure 1 are compared with the exact solution reported by Shah[3] and indicate that the Discrete Transfer method is the most accurate for the present test case.

Two-dimensional cylindrical enclosure containing an absorbing-emitting medium

The Discrete Transfer predictions were compared with experimental results obtained by Wu and Fricker[23] in a cylindrical axisymmetric furnace of the Industrial Flame Research Foundation. Predictions were also compared with Discrete Ordinates method results using S_2 and S_4 approximations[53,54].

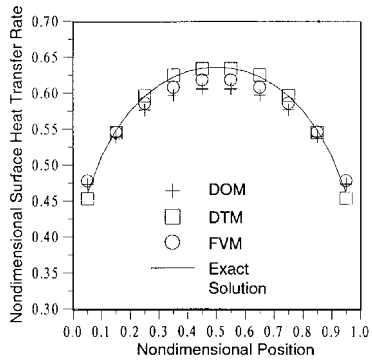

Figure 1. Comparison of non-dimensional heat fluxes predicted by different radiation models. (Taken from reference 52).

The furnace geometry, radiative properties of the medium and walls, and the measured temperatures inside the furnace are shown in Figure 2. The wall heat flux predicted using the Discrete Transfer method is compared with experimental results and with the predictions obtained with S_2 and S_4 approximations. The size of the mesh was 3×17 and 32 rays per node were used. The comparison is also shown in Figure 2 (where, for simplicity, only the S_2 and S_4 approximations obtained by Jamaluddin and Smith[54] are shown). The Discrete Transfer results clearly agree with the measured values, showing similar predictions to the discrete ordinates S_4 approximations. The peak heat flux which occurs near the burner exit is well predicted by all the methods.

Three-dimensional rectangular enclosure containing an absorbing-emitting medium

The M3 trial case (Flame 10) for the three-dimensional rectangular furnace of the International Flame Research Foundation is now considered. The data was taken from Hyde and Truelove[55] and Carvalho *et al.*[49] and is presented in Table 1 and Figure 3.

The results obtained with the Discrete Transfer method, using a $18 \times 6 \times 6$ mesh and 32 rays per node, were compared with the S_2, S_4, S_6 and S_8 discrete ordinates

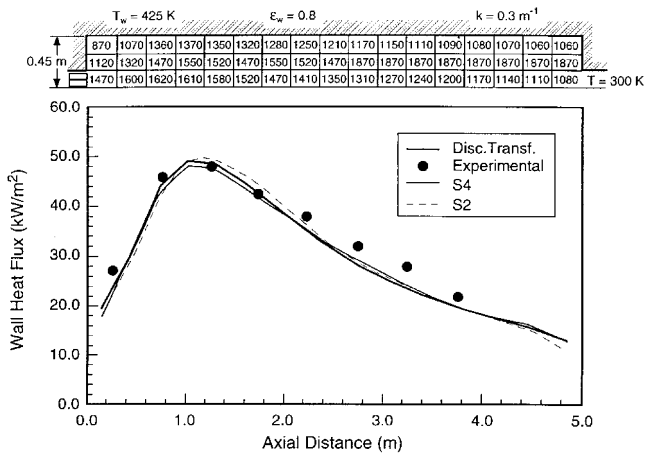

Figure 2. Wall heat flux predictions by different radiation models for the IFRF axi-symmetric furnace.

Table 1. Description of the 3-D furnace used in the IFRF M3 trials.

FURACE DIMENSIONS $6.0 \times 2.0 \times 2.0$ m		
Wall Temperatures and Emissivities		
Floor	—	$T_w = 320$ K; $\varepsilon_w = 0.86$
Sidewalls	—	
and Ceiling	—	$T_w = 1090$ K; $\varepsilon_w = 0.70$
Properties of the Medium		
T_g	=	measured (see Figure 3)
k_a	=	0.2 m^{-1}

predictions[56] and the zone model results[55]. Shown in Figure 4 are the incident radiant fluxes to the floor and the roof of the furnace. The results clearly show the good performance of the Discrete Transfer method for the calculation of heat transfer in a three-dimensional enclosure containing an absorbing-emitting medium.

Three-dimensional rectangular enclosure containing an absorbing-emitting medium with a source term

The three-dimensional absorbing-emitting case studied is based on the idealized furnace presented by Menguç and Viskanta[57]. Table 2 describes the furnace and the boundary conditions, where a finite source term was used.

The results obtained with the Discrete Transfer method, using a $10 \times 5 \times 5$ mesh and 32 rays per wall node, were compared with the discrete ordinates predictions, finite volume[52], and the zone model results[57]. The predicted gas temperature along the centrelines of the planes $x = 0.4$, 2.0 and 3.6 m is displayed in Figures 5a, 5b and 5c, respectively. The computed net heat fluxes at the south and north walls ($x = 0$ and $x = 4$ m, respectively) are shown in Figures 6a and 6b.

The gas temperatures calculated using the DOM and the diamond scheme are in good agreement with the zone method (ZM) solution at the centre of the wall but the curvature of the profile is higher. Moreover, the net flux at the south wall exhibits oscillations, and at the north wall the net flux is 5 to 6% smaller than the ZM solution. The step scheme removes the oscillations and it is in closer agreement with the ZM net heat flux at the north wall. However, it departs from the ZM net heat flux at the south wall and from the gas temperatures. The FVM results are slightly better than the DOM with the step scheme, taking the ZM solution as a reference. They are both in very good qualitative agreement with the ZM. The gas temperatures predicted by the DTM are close to the ZM solution, but the shape of the profiles reveals a peak near the centre of the wall which is not physically realistic. The net heat flux at the south wall has a small oscillation, and at the north wall the errors are larger than in other methods.

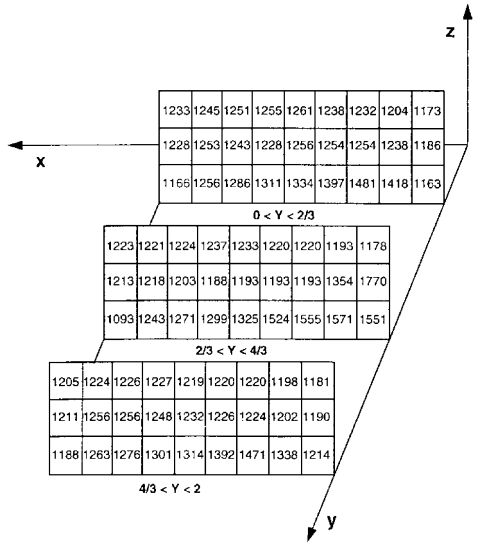

Figure 3. Measured gas temperatures (K) for the IFRF-M3 trial case (taken from Hyde and Truelove[55]).

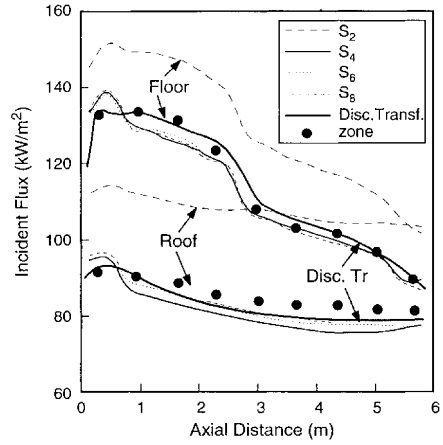

Figure 4. Predicted incident radiant fluxes to the floor and roof of the furnace.

5. RADIATIVE PROPERTIES OF COMBUSTION PRODUCTS

Combustion products can be divided into two main categories; gases, such as water vapour, carbon dioxide, carbon monoxide, nitrous oxide, and particles like soot, fuel droplets, pulverized coal, fly-ash and char. In order to apply one of the methods presented to solve the radiation heat transfer in combustion systems, it is necessary to know the radiative properties of the combustion products. In the next section, a brief presentation of the most commonly used methods in engineering problems to predict the absorption

Table 2. Description of the 3-D furnace idealized by Menguç and Viskanta[57].

FURNACE DIMENSIONS $4.0 \times 2.0 \times 2.0$ m		
Wall Temperatures and Emissivities		
Firing-end	—	$T_w = 1200$ K; $\varepsilon_w = 0.86$
exit-end	—	$T_w = 400$ K; $\varepsilon_w = 0.70$
Sidewalls	—	$T_w = 900$ K; $\varepsilon_w = 0.70$
Properties of the Medium		
S	=	5.0 kW m^{-3}
k_c	=	0.5 m^{-1}
ω	=	0.7

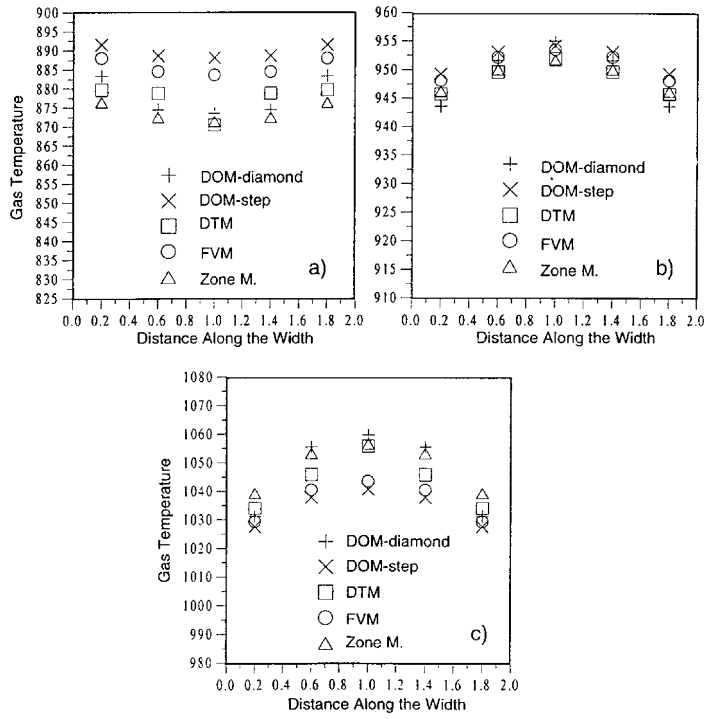

Figure 5. Predicted gas temperatures at the centre line of a) plane $x = 0.4$ m; b) plane $x = 2.0$ m; c) plane $x = 3.6$ m (taken from Coelho *et al.*[52]).

coefficient of gases will be given. Furthermore, the scattering and absorption coefficients, and the phase functions of particles will be treated emphasizing the important case of spherical particles.

Radiative Properties of Gases

Gases found in combustion processes do not scatter radiation significantly but some of them are strong absorbers and emitters (namely water vapour and carbon dioxide, amongst others). Therefore, the variation of its radiative properties with the electromagnetic spectrum must be accounted for. Spectral calculations for engineering applications are performed by dividing the wavelength spectrum into several bands. In each band the radiative characteristics (absorption and emission) are usually considered to be either uniform or to change following a pre-defined functional form. By narrowing the width of the bands, better accuracy is achieved. The most accurate approach for gas radiative transfer calculations is the line-by-line approach which consists in considering, at a given wave number, the contribution of each particular line[58,59]. However, line-by-line calculations are not practical for engineering calculations.

The following models are usually employed in engineering applications:

- Narrow-band models[60,61] (constructed from spectral absorption and emissions lines by imposing a line shape and an arrangement of lines). There are basically two line arrangements extensively used, addressed to as the Elsasser model (lines are of uniform intensity and equally spaced) and the Goody model (intensity distribution and location of lines are randomly chosen);
- Wide band models[62–65], where the profile of each band is approximated to simple shapes (triangular, box, or an exponentially decaying function can be used). The most commonly used model is the exponential wide-band model[66].
- More recently, Denison and Webb[67,68] presented a new model for predicting the radiative properties of the main gaseous species in high temperature environments denoted as the Spectral-Line Weighted-Sum-of-Gray-Gases (SLW). The parameters in the SLW model are obtained directly from the line-by-line spectra of the relevant species (e.g. H_2O and CO_2). The biggest advantage of this model is that it allows the absorption coefficient to be the basic radiative property rather than the transmissivity or emissivity. Therefore, it can be used with any arbitrary solution method for the RTE.

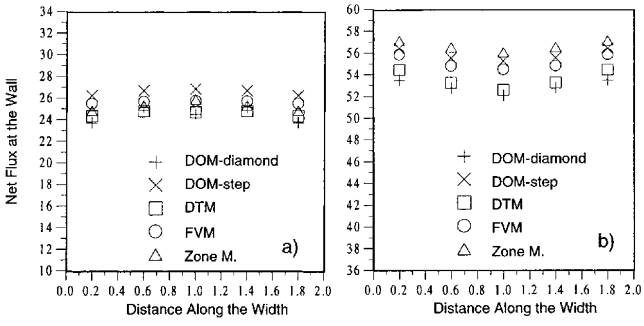

Figure 6. Predicted incident heat flux at a) the south wall; b) the north wall (taken from Coelho *et al.*[52]).

Radiative Properties of Particles

Analysis of radiation heat transfer in systems where combustion takes place usually necessitates accounting for the effects of particulates, such as soot, fuel droplets, char,

fly-ash and pulverized coal, whenever they are present in these systems. It is therefore necessary to know the radiative properties of polydispersions. These properties depend mainly on the particle size and size distribution, the value of the complex refractive index and its spectral dependency, the number density for each type of particle and the shape of the particles. Size and shape of particles are the two characteristics that commonly decide the method used to predict radiative properties.

Spherical particles

None of the particles present in the combustion products are either homogeneous or spherical. Nevertheless, in most of the situations particles can be approximated as spheres and in that case, depending on its size, specific theories can be applied.

The most extensively used model to predict the radiative properties of spherical particles is the Mie theory. Following this theory, the spectral absorption and scattering coefficients (which are the most important quantities needed for radiation heat transfer analysis) can be evaluated from:

$$k_{a,s} = \int_0^\infty \pi r^2 Q_{a,s}(x, \lambda) f(r) \mathrm{d}r \tag{16}$$

$Q_{a,s}$ is the corresponding efficiency factor, given by the Mie calculations, which depend on the size parameter ($x = 2\pi r/\lambda$) and the refractive index ($m = n + ik$), and $f(r)$ is the normalized size distribution function.

The Mie theory for spheres has been treated quite extensively by several authors[69–72] and some extension to other simple shapes like coated spheres and cylinders[71,73], elliptic cylinders[74] and spheroids have been presented—see Viskanta and Menguç[14] for a more extensive review.

When it is possible to assume that particles are spheres, although the Mie theory delivers the exact solution, there are several cases where its use can be avoided. It should be mentioned that, although the calculations for the efficiency factors of spheres are not excessively time-consuming, due to the variation of the size of the particles in space and time inside the chambers, the codes might become impractical.

It is desirable to have simple approximations for the efficiency factors. If the particles are small in size compared to the wavelength (size parameters x p 1) the following Rayleigh limit of the Mie theory expressions are obtained[69]:

$$Q_s = \frac{8}{3}\left|\frac{m^2 - 1}{m^2 + 1}\right|^2 x^4 \tag{17}$$

and

$$Q_a = -4x\, Im\left[\frac{m^2 - 1}{m^2 + 1}\right] \tag{18}$$

Due to the fact that the value of x in the Rayleigh approximation is much smaller than unity, extinction is dominated by absorption.

Unfortunately, the combustion particles that may be assumed as spheres (like fuel droplets, coal particles or char) present typical size parameters that do not fall into the Rayleigh limit. For the cases where particles have a size parameter much larger than unity the scattering is mainly a reflection process and hence can be calculated from relatively simple geometric reflection relations[71]. On the other hand, soot primary particles present size parameters usually much smaller than unity. Nevertheless, the use of Rayleigh theory can be questionable because only at the beginning of soot formation do soot particles appear as individual spherelike units. In a relatively early stage of formation, soot particles tend to agglomerate forming large branched chain-like structures that act like fractal material[75–77]. However, the optical size parameter for the relevant wavelengths (i.e. infrared) in the radiative heat transfer within combustion chambers is still small thus Rayleigh theory can be applied. Otherwise, an alternative approach that takes into account the fractal nature of these agglomerates is the Rayleigh-Debye-Gans theory for Fractal Aggregates—RDG-FA[78–82]. Figure 7 illustrates the different approaches used to model the radiative properties of spherical particles according to the size of the particles and the dimension of the refractive index of the particles.

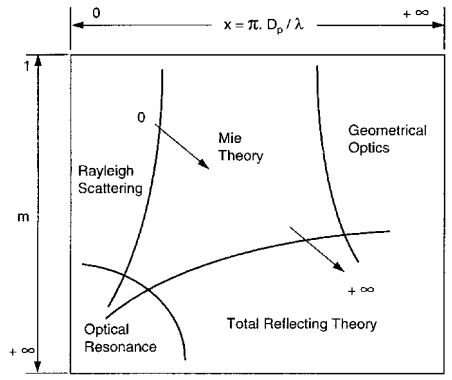

Figure 7. Different approaches used to model the radiative properties of spherical particles according to size and refractive index.

Phase functions

In most of the combustion chambers where particles exist, scattering of radiation by particles must be properly accounted for. The out-scattering term present in the RTE, equation (1), can be easily calculated if the scattering coefficient is known. Nevertheless, for the evaluation of the in-scattering term, the phase function needs to be known. The phase function, along with other radiative properties, can be obtained either through the exact solution of Maxwell's equations (for simple shapes like spheres or cylinders) or from some approximation. A convenient way of calculating the phase functions is obtained through the expansion in a series of Legendre polynomials:

$$\Phi_{(\theta,\phi)} = \sum a_n P_n(\theta, \phi) \tag{19}$$

where P_n is the Legendre polynomial of degree n and a_n a coefficient that can be obtained by the orthogonality relations of Legendre polynomials. For $n = 0$, the phase functions becomes unity which stands for isotropic scattering. For $N = 1$ the linear anisotropic phase functions appears:

$$\Phi(\theta) = 1 + a_1 \cos\theta \tag{20}$$

For $n = 2$ the phase functions represent the second degree anisotropic scattering. For the special case of $a_1 = 0$ and $a_2 = 0.5$, the Rayleigh scattering phase function appears. Most of the particles encountered in combustion chambers

scatter radiation predominantly in the forward direction. Such a scattering behaviour can be modelled using a Dirac delta function. The delta-Eddington approximation is commonly used which is written as[83]:

$$\Phi_\lambda(\theta) = 2f_\lambda \delta(1 - \cos\theta) + (1 + f_\lambda)(1 + 3g_\lambda \cos\theta) \tag{21}$$

where f and g are related to the expansion coefficients a_n.

In summary, most particles found in combustion chambers exhibit complex geometries and a wide variety of sizes and refractive indices. Therefore, further research is required in order to produce a tractable way of including these effects in practical applications. However, from an engineering point of view, small particles (when compared with the relevant wavelength) such as soot can be treated using the Rayleigh theory, while the radiative properties of larger particles like coal or fuel droplets (with a spherical shape) can be calculated using the well known Mie theory.

6. CONCLUSIONS

The paper presents a review of methods used in engineering to predict radiative heat transfer in combustion chambers. The paper is mainly divided in two parts. The first part concentrates on a description of radiation models, where special attention is given to the Discrete Transfer, Discrete Ordinates and Finite Volume methods. The performance of the most commonly used models is analysed and compared for a variety of well established test cases, including two and three-dimensional rectangular and cylindrical enclosures. From an engineering point of view, it can be concluded that the existing radiation models are satisfactory at least for non-scattering situations. However, its application to combustion chambers requires knowledge of the radiative properties of the combustion gases and particulates.

The second part of the paper deals with the methods used to predict the radiative properties (i.e. absorption, scattering coefficients and phase function) of the participating media found in combustion products. While knowledge of the spectral variation of the radiative properties of gaseous species appears to be a well known subject, modelling of the radiative properties of particles continues to be a major problem within the radiation field. In fact, particle size, shape, refractive index and morphology along with the respective distribution functions require further research in order to produce a tractable way of including these effects in practical applications.

REFERENCES

1. Siegel, R. and Howell, J. R., 1981, *Thermal Radiation Heat Transfer*, 2nd Ed. (Hemisphere, Washington DC).
2. Modest, M. F., 1993, *Radiative Heat Transfer* (McGraw-Hill).
3. Shah, N. G., 1979, New method of computation of radiation heat transfer in combustion chambers, *PhD Thesis* (Imperial College of Science and Technology, London).
4. Lockwood, F. C. and Shah, N. G., 1981, A new radiation solution method for incorporation in general combustion prediction procedures, *18th Symp (Int) on Combustion* (The Combustion Institute) pp 1405–1414.
5. Carlson, B. G. and Lathrop, K. D., 1968, Transport theory—the method of discrete ordinates, *Computing Methods in Reactor Physics*, Greenspan, H. Kelber, C. N. and Okrent, D. (eds). (Gordon & Breach, New York).
6. Fiveland, W. A., 1984, Discrete-ordinates solutions of the radiative transport equation for rectangular enclosures, *J Heat Transfer*, 106: 699–706.
7. Raithby, G. D. and Chui, E. H., 1990, A finite-volume method for predicting radiant heat transfer in enclosures with participating media, *J Heat Transfer*, 112: 415–423.
8. Chai, J. C., Lee, H. S. and Patankar, S. V., 1994, Finite volume method for radiation heat transfer, *J Thermophysics and Heat Transfer*, 8: 419–425.
9. Crosbie, A. L. and Dougherty, R. L., 1981, Two-dimensional radiative transfer in a cylindrical geometry with anisotropic scattering, *J Quant Spectrose Radiat Transfer*, 25: 551–569.
10. Dua, S. S. and Cheng, P., 1975, Multi-dimensional radiative transfer in non-isothermal cylindrical media with non-isothermal bounding walls, *Int J Heat Mass Transfer*, 18: 245–259.
11. Crosbie, A. L. and Schrenker, R. G., 1982, Exact expressions for radiative transfer in a three-dimensional rectangular geometry, *J Quant Spectrosc Radiat Transfer*, 28(6): 507–526.
12. Crosbie, A. L. and Farrell, J. B., 1984, Exact formulation of multiple scattering in a three-dimensional cylindrical geometry, *J Quant Spectrosc Radiat Transfer*, 131(5): 397–416.
13. Selçuk, N., 1985, Exact solutions for radiative heat transfer in box-shaped furnaces, *Trans ASME—J Heat Transfer*, 107: 648–655.
14. Viskanta, R. and Mengüç, M. P., 1987, Radiation heat transfer in combustion systems, *Progress in Energy Combustion Science*, 13: 97–160.
15. Howell, H. C., 1988, Thermal radiation in participating media: the past, the present, and some possible future, *Trans ASME*, 110: 1220–1229.
16. Hottel, H. C. and Cohen, E. S., 1958, Radiant heat exchange in a gas filled enclosure: allowance for non-uniformity in temperature, *AICheJ*, 4(1): 3.
17. Hottel, H. C. and Sarofim, A. F., 1967, *Radiative Transfer* (McGraw-Hill, New York).
18. Johnson, T. R. and Beer, J. M., 1972, Radiative heat transfer in furnaces—further development of the zone method of analysis, *14th Symp Int on Combustion*, p. 639.
19. Hottel, H. C. and Sarofim, A., 1972, The status of calculations of radiation from non-luminous flames, *4th Symp on Flames and Industry.*
20. Lowes, T. M., Bartelds, H., Heap, M. P., Michelfelder, S. and Pai, B. R., 1973, Prediction of radiant heat flux distribution, *IFRF Doc. GO2/A/26.*
21. Richter, W. and Quack, R., 1974, A mathematical model of a low-volatile pulverised fuel flame, *Heat Transfer in Flames*, Afgan, N. H. and Beer, J. M. (Eds) (Scripta, Book Co, Washington DC) 95–110.
22. Steward, F. R. and Cannon, P., 1971, The calculation of radiative heat flux in a cylindrical furnace using Monte Carlo model, *Int J Heat Mass Transfer*, 14: 245.
23. Wu, H. L. and Fricker, N., 1971, An investigation of the behaviour swirling jet flames in a narrow cylindrical furnace, *2nd Members Conf* (Industrial Flame Research Foundation, Ijmuiden, The Netherlands).
24. Heap, M. P., Bartelds, H., Lowes, T. M. and Michelfelder, 1974, Prediction of radiant heat flux distribution, *Heat Transfer in Flames*, Afgan, N. H. and Beer, J. M. (Eds) (Scripta Book Co, Washington DC).
25. Selçuk, N., Siddal, R. G. and Beer, J. M., 1976, A comparison of mathematical models of the radiative behaviour of a large-scale experimental furnace, *16th Symp Int on Combustion*, p. 53.
26. Howell, J. R. and Perlmutter, M., 1964, Monte Carlo solution of thermal transfer through radiant media between gray walls, *J Heat Transfer*, 86: 116.
27. Taniguchi, H., Kudo, K., Hyaasaka, H., Yang, W. and Tashiro, H., 1984, *Fundamentals of Thermal Radiation Heat Transfer*, Min, T. and Chen, J. (Eds) *ASME HTD*, 40: 29–36.
28. Hamaker, H. C., 1947, Philips Research Repts., 3, 103, 112 and 142.
29. Gosman, A. D. and Lockwood, F. C., 1973, Incorporate of a flux model for radiation into a finite difference procedure for furnace calculations, *14th Symp (Int) on Combustion* (The Combustion Institute) 661.
30. Patankar, S. V. and Spalding, D. B., 1974, Simultaneous predictions of flow pattern and radiation for three-dimensional flames, *Heat Transfer in Flames*, Afgan N. H. and Beer, J. M. (Eds) (Scripta Book Co, Washington DC) 73–94.
31. Abramzon, M. N. and Lisin, F. N., 1984, *High Temp*, 22: 95.
32. Spalding, D. B., 1970, Personal Notes.
33. Siddall, R. G. and Selçuk, N., 1976, Two-flux modelling of two-dimensional radiative transfer in axi-symmetrical furnaces, *J Inst Fuel*, 49: 10–20.
34. Siddall, R. G. and Selçuk, N., 1979, Evaluation of a new six-flux model

for radiative transfer in rectangular enclosures, *Trans IChemE*, 57: 163–169.
35. Jeans, J. H., 1917, The equations of radiative transfer of energy, *Monthly Notes, Royal Astron Soc*, 78: 28.
36. Viskanta, R., 1966, Radiative transfer and interaction of convection with radiation heat transfer, *Advances in Heat Transfer*, Irvine and Hartnett (Eds), Vol 3: 175–252.
37. Higenyi, J. and Bayazitoglu, Y., 1980, Differential approximation of radiactive heat transfer in a gray medium, *J Heat Transfer*, 102: 719–723.
38. Whitacre, G. R. and McCann, R. A., 1975, Comparison of methods for the prediction of radiant heat flux distribution and temperature, *ASME paper*, 75-HT-9.
39. Chandrasekhar, S., 1960, *Radiative Transfer* (Dover Publication, New York).
40. Truelove, J. S., 1976, An evaluation of the discrete ordinates approximation of radiative transfer in an absorbing, emitting and scattering planar medium (UK Atomic Energy Commission, Hartwell) *Rept.—AERE R8478*.
41. Carvalho, M. G., Durão, D. F. G. and Pereira, J. C. F., 1987, Prediction of the flow, reaction and heat transfer in an oxy-fuel glass furnace, *Int J Eng Computations*, 4(1): 23–34.
42. Gosman, A. D., Lockwood, F. C., Megahed, I. E. A. and Shah, N. G., 1980, The prediction of the flow, reaction and heat transfer in the combustion chamber of a glass furnace, *AIAA18th Aerospace Sciences Meeting, January 14, Pasadena, CA, USA.*
43. Carvalho, M. G., Nogueira, M. and Wang, J., 1995, *Verre*, 1(5): 9–13.
44. Lankhorst, A. M., Muysenberg, H. P. H. and Sanders, M. P. J., Coupled combustion modelling and glass tank modelling in oxy- and air-fired glass-melting furnaces.
45. Carvalho, M. G. and Coelho, P. J., 1989, Heat transfer in gas turbine combustors, *AIAA—J Thermophysics and Heat Transfer*, 3(2): 123.
46. Fiveland, W. A. and Wessel, R., 1986, FURMO: A numerical model for predicting performance of three-dimensional pulverized-fuel fired furnaces, *ASME Paper 86-HT-35.*
47. Dinho, P., Coelho, L. R., Azevedo, J. and Carvalho, M. G., 1994, Modelling radiation in pulverized coal combustion, *Proc Eurotherm Seminar* #37*–Heat Transfer in Radiating and Combustion Systems—2 Saluggia, Italy.*
48. Boyd, R. K. and Kent, J. H., 1986, Three dimensional furnace computer modelling, *21 Symp (Int) on Combustion* (The Combustion Inst., Pittsburgh, PA) pp. 265–274.
49. Carvalho, M. G., Farias, T. and Fontes, P., 1991, Predicting radiating heat transfer in absorbing emitting, and scattering media using the discrete transfer method, ASME—HTD-Vol. 160, *Fundamentals of Radiation Heat Transfer*, pp. 17–26.
50. Carvalho, M. G., Farias, T. and Fontes, P., 1993, Multidimensional modeling of radiative heat transfer in scattering media, *J Heat Transfer*, 115: 486–489.
51. Coelho, P. J. and Carvalho, M. G., 1997), A conservative formulation of the discrete transfer method, *J Heat Transfer*, 119: 118–128.
52. Coelho, P. J., Gonçalves, J. M. and Carvalho, M. G., 1995, A comparative study of radiation models for coupled fluid flow/heat transfer problems, *Proc 9th Int Conf for Numerical Methods in Thermal Problems*, Lewis, R. W. and Dubertaki, P. (Eds) (Pineridge Press, Swansea) Vol. IX, part 1, pp. 378–389.
53. Fiveland, W. A., 1986, A discrete-ordinates method for predicting radiative heat transfer in axisymmetric enclosures, *ASME paper 82-HT-20.*
54. Jamaluddin, A. S. and Smith, P. J., 1988, Predicting radiative transfer in axisymmetric cylindrical enclosures using the discrete ordinates method, *Comb Sci Technol*, 62: 173.
55. Hyde, D. J. and Truelove, J. S., 1977, The discrete ordinates approximate for multi-dimensional radiant heat transfer in furnace, *AERE R-8502* (AERE Harwell, UK).
56. Jamaluddin, A. S. and Smith, P. J., 1988, Predicting radiative transfer in rectangular enclosures using the discrete ordinates method, *Comb Sci Technol*, 59: 321–340.
57. Mengüç, M. P. and Viskanta, R., 1985, Radiative transfer in three-dimensional rectangular enclosures containing inhomogeneous anisotropically scattering media, *J Quant Spectrosc Rad Trans*, 33: 533–549.
58. Hartmann, J. M., Rosenmann, L., Perrin, M. Y. and Taine, J., 1988, Accurate calculated tabulations of CO line broadening by H_2O, N_2, O_2 and CO_2 in the 200–3000 K temperature range, *Applied Optics*, 27(15).
59. Rosenmann, L., Hartmann, J. M., Perrin, M. Y. and Taine, J., 1988, Accurate calculated tabulations of IR and Raman CO_2 line broadening by CO_2; H_2O, N_2, O_2 in the 300–2400-K temperature range, *Applied Optics*, 27(18).
60. Goody, R. M., 1964, *Atmosphere Radiation* (Oxford University Press, London).
61. Tien, C. L., 1968, *Advances in Heat Transfer*, Irvine, Jr., T. F. and Hartnett, J. P. (Eds), Vol. 5, pp 254–324 (Academic Press, New York).
62. Tien, C. L. and Lowder, J. E., 1966, *Int J Mass Transfer*, 9: 698.
63. Hsieh, T. C. and Greif, R., 1972, Theoretical determination of the absorption coefficient and the total band absorptance including a specific application to carbon monoxide, *Int J Heat Mass Transfer*, 15: 1477–1487.
64. Edwards, D. K. and Balakrishnan, A., 1973, Thermal radiation by combustion gases, *Int J Heat Mass Transfer*, 16: 25–40.
65. Felske, J. D. and Tien, C. L., 1974, Shorter communication: A theoretical closed form expression for the total band absorptance of infrared-radiating gases, *Int J Heat Mass Transfer*, 17: 155–158.
66. Edwards, D. K. and Menard, W. A., 1964, *Applied Optics*. 3: 621.
67. Denison, M. K. and Webb, B. W., 1993, A spectral line based weighted-sum-of-grey-gases model for arbitrary RTE solvers, *ASME J Heat Transfer*, 115: 1004–1012.
68. Denison, M. K. and Webb, B. W., 1995, The spectral line based weighted-sum-of-grey-gases model in non-isothermal non-homogeneous media, *ASME J Heat Trans*, 177: 359–365.
69. Van de Hulst, H. C., 1957, *Light Scattering by Small Particles* (Wiley, New York, [also Dover, New York, 1981]).
70. Kertker, M., 1969, *The Scattering of Light* (Academic Press, New York).
71. Bohren, C. F. and Huffman, D. R., 1984, *Absorption and Scattering of Light by Small Particles* (Wiley, New York).
72. Dave, J. V., 1968, Subroutines for computing the parameters of the electromagnetic radiation scattered by a sphere, *IBM J Res*, No. 320–3237.
73. Mackowski, D. W., Altenkirch, R. A. and Menguç, M. P., 1987, Extinction and absorption coefficients of cylindrically-shaped soot particles, *Comb Sci Technol*, 53: 399–410.
74. Yeh, C., 1965, Backscattering cross section of a dielectric elliptical cylinder, *J Opt Soc Am*, 55(3), 390.
75. Köylü, Ü. Ö. and Faeth, G. M., 1992, Structure of overfire soot in buoyant turbulent diffusion flames at long residence times, *Combust Flame*, 89: 140–156.
76. Megaridis, C. M., Dobbins, R. A., 1990, Morphological description of flame-generated materials, *Comb Sci Technol*, 71: 95.
77. Köylü, Ü.Ö., Faeth, G. M., Farias, T. L. and Carvalho, M. G., 1995, Fractal and projected structure properties of soot aggregates, *Combustion and Flame*, 110: 621–633.
78. Köylu, Ü. Ö. and Faeth, G. M., 1993, Radiation properties of flame-generated soot, *J Heat Trans*, 115: 409–417.
79. KöyÏü, Ü. Ö. and Faeth, G. M., 1994, Optical properties soot in buoyant turbulent diffusion flames at long residence times, *J Heat Trans*, 116: 152–159.
80. Köylü, Ü. Ö. and Faeth, G. M., 1994, Optical properties of soot in buoyant laminar diffusion flames at long residence times, *J Heat Trans*, 116: 152–159.
81. Farias, T. L., Köylü, Ü. Ö. and Carvalho, M. G., 1996, Effects of polydispersity of aggregates and primary particles on radiative properties of simulated soot, *J Quant Spect and Rad Trans*, 55(3): 357–371.
82. Farias, T. L., Köylü, Ü. Ö. and Carvalho, M. G., 1996, The range of validity of the Rayleigh-Debye-Gans/fractal-aggregate theory for computing optical properties of fractal-like aggregates, *Applied Optics*, 35(33): 6560–6567.
83. Crosbie, A. L. and Davidson, G. W., 1985, Dirac-delta function approximation to the scattering phase function, *J Quant Spectr Rad Trans*, 33: 391–409.

ADDRESS

Correspondence concerning this paper should be addressed to Professor M. da Graça Carvalho, Department of Mechanical Engineering, Instituto Superior Tecnico, Technical University of Lisbon, Av Rovisco Pais, 1096 Lisboa Codex, Portugal.

This paper was presented at the 5th UK National Heat Transfer Conference, held at Imperial College, London 17–18 September 1997.